Mesoporous Silica with Large Entrances

Cubic Mesoporous Silica with Large Controllable Entrance Sizes and Advanced Adsorption Properties**

Jie Fan, Chengzhong Yu, Feng Gao, Jie Lei, Bozhi Tian, Limin Wang, Qian Luo, Bo Tu, Wuzong Zhou, and Dongyuan Zhao**

Recently, mesoporous materials have attracted much attention because of their emerging applications in catalysis, adsorption, sensors, and separations.[1] It is generally accepted

[*] Dr. C. Yu, Prof. Dr. D. Zhao, J. Fan, F. Gao, J. Lei, B. Tian, L. Wang, Q. Luo, B. Tu
Shanghai Key Laboratory of Molecular Catalysis and Innovative Materials
Department of Chemistry
Fudan University
Shanghai 200433 (P. R. China)
Fax: (+86) 21-6564-1740
E-mail: czyu@fudan.edu.cn
dyzhao@fudan.edu.cn
Dr. W. Zhou
School of Chemistry
University of St. Andrews
St. Andrews, Fife KY16 9ST (UK)

[**] Supported by the National Science Foundation of China (29925309 and 20233030), State Key Research Program (G2000048001 and 2002AA321010), Shanghai Science Committee (0212nm043).

Supporting information for this article is available on the WWW under http://www.angewandte.org or from the author.

  DOI: 10.1002/ange.200351027

that mesoporous materials with 3D pore systems exhibit more advantages in mass diffusion and transportation compared with MCM-41 materials[2,3] containing 1D channels. Cubic mesoporous silicas MCM-48 (*Ia-3d*),[2,3] SBA-1 (*Pm-3n*),[4] SBA-16 (*Im-3m*),[5] FDU-1,[6] and SBA-2,[4,7] SBA-12[5,8] with 3D hexagonal structures ($P6_3/mmc$) have been synthesized. FDU-1 was originally reported to have a body-centered cubic structure (*Im-3m*). Very recently it was suggested based on high-resolution transmission electron microscopy (HRTEM) and small-angle X-ray scattering that FDU-1 silica synthesized under typical conditions was a face-centered cubic structure (*Fm-3m*) with 3D hexagonal mesophase intergrowth.[9] Such intergrowth is also common in SBA-2[7] and SBA-12.[8] However, a pure face-centered cubic (*Fm-3m*) mesoporous material without intergrowth has not been reported yet. Except for MCM-48 material with a bicontinuous pore structure and a cubic (*Im-3m*) mesostructure with possible bicontinuous "Plumber's Nightmare" pore morphology,[10] most of these cubic and 3D hexagonal mesoporous materials have cagelike pore structures, in which relatively large cavities are connected by some pore entrances with smaller sizes (also referred to as windows or connectivities in some literatures, see Figure 1). Gas sorption analysis method

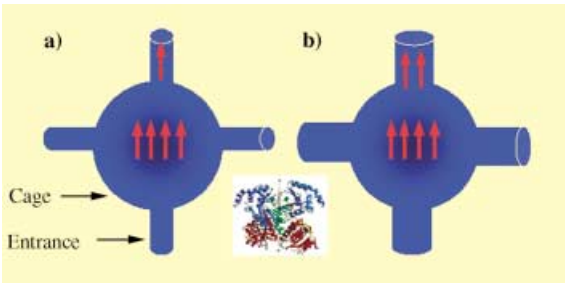

Figure 1. Schematic drawing of the cavity and entrance of a cagelike mesoporous material with similar cavity sizes but different entrance sizes, a) small entrances, b) large entrances. The diffusion rates of enzymes (inset of Figure 1) within the cage and entrance are represented by the number of arrows.

may be applied to well define the sizes of these parameters.[11] TEM techniques have also been developed to solve the structures of both the cavities and the connectivities of mesoporous materials.[8,12]

The pore engineering of mesoporous materials is of great importance for various applications where different sizes of molecules are involved. By choosing structure-directing agents such as block copolymers, by using swelling agents, and by manipulating synthesis conditions, such as the temperature of the hydrothermal treatment, mesoporous materials with desired structures and adjustable pore sizes have been obtained.[5] In the cases of mesoporous materials with cagelike structures, much effort has been devoted to the control of the cavity size, while little work has been carried out to study another important structural parameter, the pore entrance. Jaroniec and co-workers reported the tailoring of entrance sizes in FDU-1 materials by the modification of the silica surface with monofunctional organosilane, thus the entrance sizes may be controlled within a certain range (5.0–1.2 nm).[13] However, such small entrance sizes of mesoporous materials may limit their uses in protein adsorption and separation processes.[14,15] By performing hydrothermal treatment for a sufficiently long time at temperatures below 393 K, Jaroneic and co-workers also showed that the pore-entrance size of FDU-1 silica could be enlarged, but there was evidence that the distribution of the pore-entrance size was quite broad.[9]

Herein, we report our synthesis of a large cavity ($10 \approx 12.3$ nm) cubic (*Fm-3m*) mesoporous silica (denoted as FDU-12) in the presence of block copolymer templates. The size of the entrances may be adjusted in the range of $4 \approx 9$ nm as confirmed by nitrogen-sorption studies and by examining the negative replicas of gold and carbon. Most importantly, it is revealed that the entrance size of mesoporous materials is a key factor for the applications in which mass transportations and diffusions are involved, by the following observations: First, the immobilization of enzymes is facilitated for FDU-12 materials with large entrance sizes (Figure 1). Second, cubic mesoporous carbon replicas with ordered large pores (up to 9.8 nm) have been synthesized by using FDU-12 with widened entrance sizes as the hard templates. These results may add a new understanding to the correlation between structure parameters and the properties of mesoporous materials.

Mesoporous FDU-12 samples were synthesized in acidic solutions by using nonionic block copolymer $EO_{106}PO_{70}EO_{106}$ (EO is poly(ethylene oxide) and PO is poly(propylene oxide)) as a template, 1,3,5-trimethylbenzene (TMB) together with inorganic salts (e.g. KCl), as additives, and tetraethyl orthosilicate (TEOS) as the silica source. Hydrothermal treatment was performed on the resulting silica–surfactant-composite precipitates at different temperatures (designated FDU-12–X, X indicates the temperature of hydrothermal treatment). The synthesized samples were calcined at 823 K for 6 h to obtain mesoporous silica materials.

Powder X-ray diffraction (XRD) patterns of the as-synthesized and calcined FDU-12–373 specimens are shown in Figure 2. Both patterns show five well-resolved peaks, which can be assigned to the (111), (220), (311), (331) and (442) reflections of a face-centered cubic structure. There are several possibilities of the space group for FDU-12 from the extinction condition of XRD patterns, such as *Fm-3m* and *Fm-3c*. The ideal structure of FDU-12 is speculated to have a space group *Fm-3m*, as it has the highest symmetry among all possible space groups. The unit cell parameters calculated from the XRD data are 29.2 and 25.3 nm for the as-synthesized and calcined specimens, respectively. Calcination of the sample gives rise to relatively low shrinkage ($\approx 12\,\%$) and an increase of the diffraction intensity. FDU-12 is quite stable; even after higher temperature hydrothermal treatment (up to 413 K), the corresponding intensive (111) and (311) diffraction peaks for a face-centered cubic mesostructure are still observed.

TEM images of calcined FDU-12–373 materials taken along the [100] and [111] directions are shown in Figure 3a and 3b, respectively. Taken directly from the images, the unit cell parameter *a* is estimated to be 26 nm, which is in good

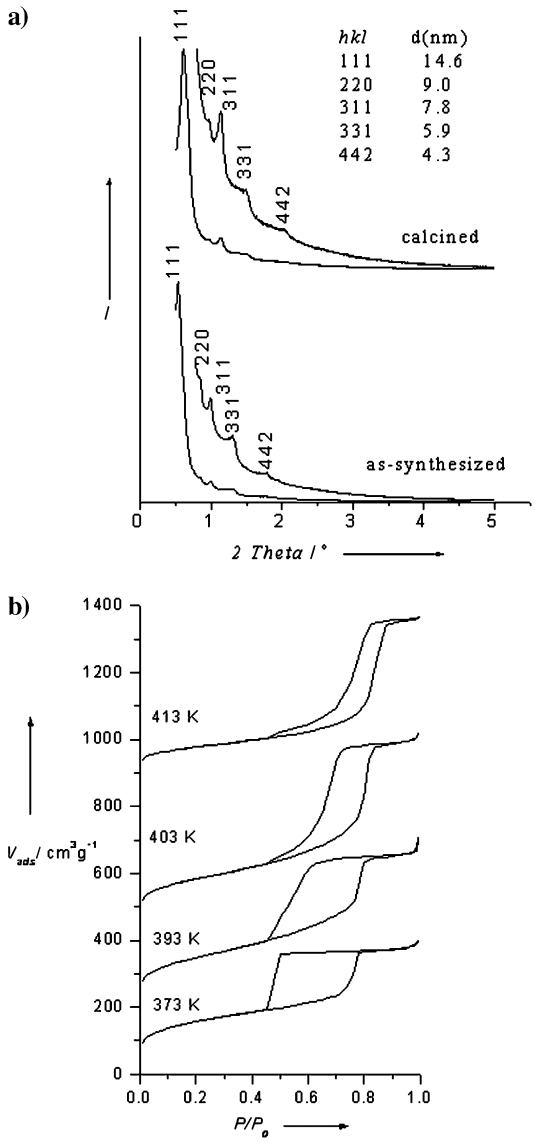

Figure 2. a) XRD patterns (I = intensity) of FDU-12–373 and b) nitrogen sorption isotherms of calcined FDU-12–X samples. The adsorption isotherms for FDU-12–393, –403, and –413 samples are shifted by 200, 450, 900 cm^3g^{-1} (STP), respectively.

accordance with the XRD results. The highly ordered lattice array over large domains under the TEM observations suggests that the FDU-12 products have a uniform, well-defined cubic mesostructure (*Fm-3m*) without intergrowth. The diameter of the cages may be directly measured from the thin edge of the particle in Figure 3a (see also Supporting Information) to be about 10.7 nm, in good accordance with the N_2 sorption results (see below). In addition, 1D-like large pores that are formed by the linear combination of many spherical cages can be further observed in the TEM images (see Supporting Information), thus implying that the calcined FDU-12 have large entrances. Scanning electron microscopy (SEM) images of the calcined FDU-12 show mostly spherical morphologies (see Supporting Information). These spherical particles have relatively uniform sizes of 2–3 μm. Different hydrothermal-treatment temperatures (373–413 K) result in little change in particle morphology.

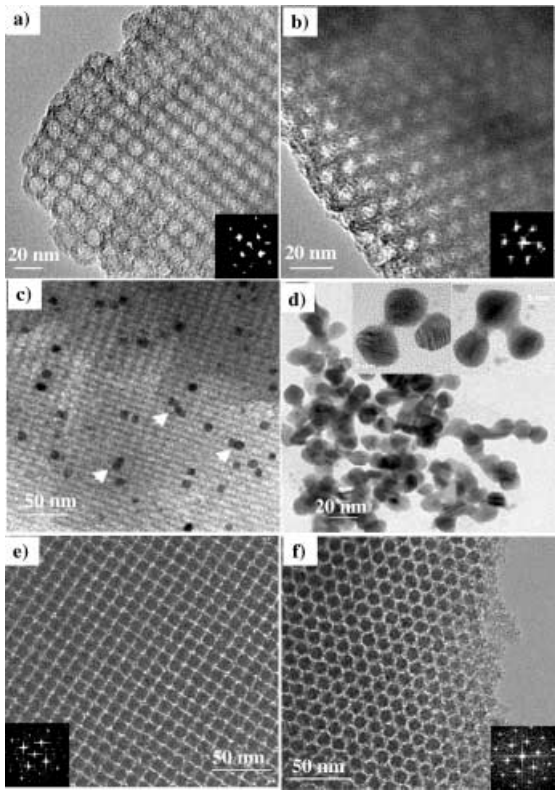

Figure 3. TEM images a) and b) of FDU-12–373 recorded along the [100] and [111] directions (Fourier diffractograms inset), respectively. TEM images c) of Au/FDU-12–403 and d) Au nanocrystals after removal of the silica frameworks. The insets show enlarged TEM images of dumbbell-like Au nanoparticles formed inside FDU-12–373 (left) and FDU-12–403 (right). TEM images e) and f) of C-FDU-12–403 viewed down the [100] and [111] directions (Fourier diffractograms inset), respectively.

Normally, a conventional large pore cagelike mesoporous silica, such as SBA-16[5] or FDU-1,[6] shows a large H_2 hysteresis loop, similar to FDU-12–373 (Figure 2b). On the other hand, no hysteresis loop is observed in SBA-1, SBA-2 and SBA-12 in which the sizes of cavities and entrances are relatively smaller.[4,5] In the case of FDU-12–X materials, it is noteworthy that the hysteresis loops become smaller with increasing temperature of the hydrothermal treatment (373 → 413 K), FDU-12–403 and FDU-12–413 materials even have typical H_1 hysteresis loops. Accordingly, the shift of desorption branches to high relative pressure indicates that the entrance sizes of FDU-12 have been enlarged. It is noteworthy that both the cavity and the entrance size distributions of FDU-12–X materials are quite narrow, as can be seen from the steep change from the adsorption and desorption branches, respectively. The sizes of the cavities and entrances as well as other physical parameters of FDU-12-X are listed in Table 1. When the hydrothermal treatment temperature is increased from 373 to 413 K, the cavity size is increased to a small extent from 10 to 12.3 nm (increasing 23%), while the entrance size is increased much more significantly from ≈4 to 8.9 nm (increasing 123%). These structural features are very important in understanding the properties of the FDU-12–X materials.

Table 1: Physicochemical properties of calcined mesoporous silica FDU-12-X.

Sample	*a* (nm)	Pore size (nm)	Entrance size (nm)	Pore volume (cm^3g^{-1})	Surface area (m^2g^{-1})
FDU-12–373	25.3	10.0[a]	≈4[b]	0.66	712
FDU-12–393	26.7	11.0[a]	5.3[a]	0.73	569
FDU-12–403	27.3	12.4[a]	7.5[a]	0.86	480
FDU-12–413	27.8	12.3[a]	8.9[a]	0.78	281

[a] Calculated from the desorption branch of the N_2 adsorption/desorption isotherms based on BJH model. [b] Estimated from the corresponding Au nanocrystal images

The cavity and entrance sizes of FDU-12–X materials have also been determined from their negative replicas of dilute Au nanocrystals. Figure 3c shows a TEM image of Au/FDU-12–403 specimen, which shows that all the Au nanoparticles are well confined in the cavities. As the loading amount of Au is quite low (3.0 wt%), it may be observed that occasionally two or three Au nanoparticles are located in neighboring cavities and connected through the entrances (indicated by small arrows). After removal of the silica frameworks, these connected Au nanoparticles show a dumbbell-like morphology (Figure 3d), which directly reveals that two cavities with ≈12 nm in diameter are connected by an entrance of ≈8 nm in size (Figure 3d, inset, right), in accordance with the sorption results. For comparison, the entrance size of FDU-12–373 is about 4 nm estimated from the Au TEM image (Figure 3d, inset, left), smaller than that of FDU-12–403, but still larger than that of conventional SBA-16 materials (≈2.3 nm).[12] It is noted that FDU-12–413 materials have the largest uniform entrance size among all known ordered mesoporous materials with cagelike structures.

By using the same structure-directing agents, cubic mesoporous materials SBA-16 (*Im-3m*) were synthesized by Stucky and co-workers.[5] In our experiments, inorganic salts were employed to increase the interaction of the silicate species with nonionic block copolymers, thus resulting in highly ordered products.[16] A swelling agent, TMB, was used to enlarge the entrance and cavity sizes.[17] The organic TMB may also enter the hydrophobic part of micelles and increase the volume ratio of the hydrophobic core, leading to a phase transformation from the body-centered cubic structure (*Im-3m*) to a more closely packed face-centered cubic structure (*Fm-3m*).[18] The careful manipulating of different synthesis conditions has led to the successful synthesis of FDU-12 mesoporous materials with enlarged pore entrance sizes.

The immobilization of proteins is of great importance for applications such as biosensors and biocatalysis. Recently, mesoporous silica was shown to be a more promising material in bioimmobilization in comparison with conventional sol–gels because of their uniform pore size, large surface area, pore volume and opened pore structures.[19,20] The advantage of widening the size of the pore entrances of mesoporous materials with cubic cagelike structures was reflected in the immobilization of proteins within the FDU-12–X materials. Lysozyme with an average spherical diameter of ≈3.2 nm was used to examine the protein immobilization ability of FDU-12. Over the same period of contact time, lysozyme was adsorbed increasingly into FDU-12 with increasing entrance sizes (Figure 4). Furthermore, the time for lysozyme adsorbed within FDU-12 to reach the equilibrium was also found to depend strongly on the size of the entrances. The fast equilibrium (4 hours) was observed for the FDU-12–413 and FDU-12–403 with large entrances, whereas it took more than three days to reach the equilibrium for FDU-12–373 silica with relatively smaller entrances. For comparison, SBA-16 materials with the smallest entrances[5] have the lowest lysozyme adsorption and longest equilibrium time. As the particle size, pore volume and pore size vary only in a small range for FDU-12–X materials, and the surface area of FDU-12–413 is the smallest among all samples; the observed difference for the immobilization property in parallel experiments may be mostly attributed to the differences of the entrance sizes of the FDU-12–X materials.

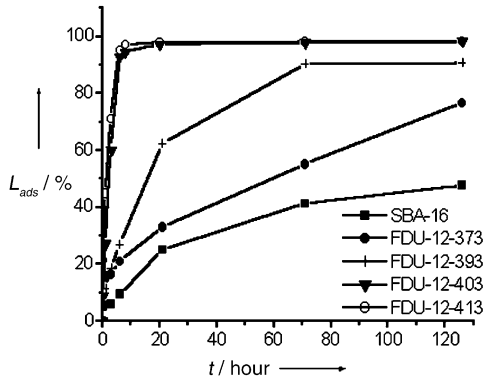

Figure 4. Adsorption of lysozyme within caged mesoporous silicas as a function of contact time. L_{ads} = lysozyme adsorbed amount (W:W).

Mesoporous FDU-12 materials with large entrances are also found to be more suitable hard templates for the synthesis of ordered nanoporous carbon than conventional SBA-16 materials. TEM (Figure 3e and f), XRD and nitrogen sorption results (see Supporting Information) show that the carbon replica, C-FDU-12–403, synthesized from the FDU-12–403 templates have well ordered mesostructures (*Fm-3m*), while the structural order of mesoporous carbon synthesized from the traditional SBA-16 templates with smaller entrances (≈2.3 nm)[12] is quite poor (see Supporting Information). The cell parameter *a* of C-FDU-12–403 calculated from XRD and TEM is 23.9 and 22.7 nm, respectively. The relatively smaller cell parameter of C-FDU-12–403 compared to that of its silica template FDU-12–403 (27.3 nm) may be attributed to the high temperature treatment during the replication process. TEM images of FDU-12–X and the corresponding C-FDU-12–X materials viewed along the same directions show reverse contrast. The pore size of C-FDU-12–X can reach 9.8 nm when FDU-12–373 is applied as the hard template (Supporting Information) calculated by using the BJH method, the largest among all reported cubic ordered

mesoporous carbon materials. These large-pore mesoporous carbon with interconnected networks is of great importance for various applications including electrodes for supercapacitors, sensors for large biomolecules and the adsorption of bulky pollutants.[21]

In summary, large pore face-centered cubic (*Fm-3m*) mesoporous silicas FDU-12–X without intergrowth with other phases have been synthesized by using nonionic block copolymer templates. The entrance sizes of these materials can be continuously tailored (4–9 nm). Most importantly, this work shows that the entrance size of mesoporous materials with cagelike structures is a key factor for the applications in which mass transportation and diffusion are necessary. Such large pore materials with enlarged entrance sizes have proven to be much useful in protein adsorption and carbon replica processes.

Experimental Section

In a typical synthesis, 2.0 g of triblock copolymers $EO_{106}PO_{70}EO_{106}$ (F127, BASF), 2.0 g of TMB and 5.0 g of KCl were dissolved in 120 mL of 2 M HCl and stirred for 24 h. TEOS (8.3 g) was added to the resulting reaction mixture, which was left to stir for a further 24 h at 313 K before being transferred to an autoclave and heated at the desired temperature for 72 h. The solid product was collected by filtration and dried at room temperature in air. The resulted silica/surfactant composite powder was calcined at 823 K for 6 h to obtain mesoporous silica.

The Au nanocrystals were prepared by using FDU-12–X as the hard templates according to a reported method.[22] Kinetic experiments to determine the amount of lysozyme adsorbed into the mesoporous materials as a function of contact time were conducted by mixing 4 mL of 1.0 mg mL^{-1} protein solution (potassium phosphate as buffer at pH 7.0) with 40 mg of mesoporous silica under stirring at 20 °C in a vessel covered to prevent evaporation. Samples were withdrawn periodically for immediate analysis and then returned to the mixture. Adsorbed amounts were calculated from the difference of concentrations of the enzyme before and after adsorption measured by UV spectroscopy at 280 nm. The synthesis of mesoporous carbon (denoted as C-FDU-12-X) is similar to that reported by Ryoo and co-workers except for difference of silica-to-sucrose ratios.[23]

Received: January 27, 2003
Revised: May 7, 2003 [Z51027]

Keywords: adsorption · carbon · enzymes · mesoporous materials · silica

[1] M. E. Davis, *Nature* **2002**, *417*, 813.
[2] C. T. Kresge, M. E. Leonowicz, W. J. Roth, J. C. Vartuli, J. S. Beck, *Nature* **1992**, *359*, 710.
[3] J. S. Beck, J. C. Vartuli, W. J. Roth, M. E. Leonowicz, C. T. Kresge, K. D. Schmitt, C. T. W. Chu, D. H. Olson, E. W. Sheppard, et al. , *J. Am. Chem. Soc.* **1992**, *114*, 10834.
[4] Q. S. Huo, D. I. Margolese, G. D. Stucky, *Chem. Mater.* **1996**, *8*, 1147.
[5] D. Zhao, Q. Huo, J. Feng, B. F. Chmelka, G. D. Stucky, *J. Am. Chem. Soc.* **1998**, *120*, 6024.
[6] C. Yu, Y. Yu, D. Zhao, *Chem. Commun.* **2000**, 575.
[7] W. Z. Zhou, H. M. A. Hunter, P. A. Wright, Q. F. Ge, J. M. Thomas, *J. Phys. Chem. B* **1998**, *102*, 6933.
[8] Y. Sakamoto, I. Diaz, O. Terasaki, D. Y. Zhao, J. Perez-Pariente, J. M. Kim, G. D. Stucky, *J. Phys. Chem. B* **2002**, *106*, 3118.
[9] J. R. Matos, M. Kruk, L. P. Mercuri, M. Jaroniec, L. Zhao, T. Kamiyama, O. Terasaki, T. J. Pinnavaia, Y. Liu, *J. Am. Chem. Soc.* **2003**, *125,* 821.
[10] A. C. Finnefrock, R. Ulrich, A. Du Chesne, C. C. Honeker, K. Schumacher, K. K. Unger, S. M. Gruner, U. Wiesner, *Angew. Chem.* **2001**, *113,* 1247; *Angew. Chem. Int. Ed.* **2001**, *40*, 1207.
[11] M. Kruk, M. Jaroniec, *Chem. Mater.* **2001**, *13*, 3169.
[12] Y. H. Sakamoto, M. Kaneda, O. Terasaki, D. Y. Zhao, J. M. Kim, G. Stucky, H. J. Shim, R. Ryoo, *Nature* **2000**, *408*, 449.
[13] M. Kruk, V. Antochshuk, J. R. Matos, L. P. Mercuri, M. Jaroniec, *J. Am. Chem. Soc.* **2002**, *124*, 768.
[14] Y. J. Han, G. D. Stucky, A. Butler, *J. Am. Chem. Soc.* **1999**, *121*, 9897.
[15] J. W. Zhao, F. Gao, Y. L. Fu, W. Jin, P. Y. Yang, D. Y. Zhao, *Chem. Commun.* **2002**, 752.
[16] C. Z. Yu, B. Z. Tian, J. Fan, G. D. Stucky, D. Y. Zhao, *J. Am. Chem. Soc.* **2002**, *124*, 4556.
[17] J. Fan, C. Z. Yu, L. M. Wang, B. Tu, D. Y. Zhao, Y. Sakamoto, O. Terasaki, *J. Am. Chem. Soc.* **2001**, *123*, 12113.
[18] J. M. Kim, Y. Sakamoto, Y. K. Hwang, Y. U. Kwon, O. Terasaki, S. E. Park, G. D. Stucky, *J. Phys. Chem. B* **2002**, *106*, 2552.
[19] J. Deere, E. Magner, J. G. Wall, B. K. Hodnett, *Chem. Commun.* **2001**, 465.
[20] J. Deere, E. Magner, J. G. Wall, B. K. Hodnett, *J. Phys. Chem. B* **2002**, *106*, 7340.
[21] J. Lee, K. Sohn, T. Hyeon, *J. Am. Chem. Soc.* **2001**, *123*, 5146.
[22] Y. J. Han, J. M. Kim, G. D. Stucky, *Chem. Mater.* **2000**, *12*, 2068.
[23] S. Jun, S. H. Joo, R. Ryoo, M. Kruk, M. Jaroniec, Z. Liu, T. Ohsuna, O. Terasaki, *J. Am. Chem. Soc.* **2000**, *122*, 10712.

